

SERI QUARTERLY REPORT NO. 4

(Period of 1 JAN -- 31 MARCH 1980)

CONTRACT: SERI XP-9-8081-1  
"Materials for High Efficiency Monolithic  
Multigap Concentrator Solar Cells"  
Period of 1 January -- 31 March 1980

CONTRACTOR: Varian Associates, Inc.  
611 Hansen Way  
Palo Alto, CA 94303

The objectives of this work are to develop a materials technology of the AlGaInAs and AlInAsSb mixed crystal systems. These technologies are directed towards the development of a two-gap, monolithic, lattice-matched concentrator cell with 28% or higher AM2 conversion efficiency at 500 to 1000 suns.

The work to be performed is subdivided into the five major tasks outlined below.

Task 1. Develop and demonstrate the technology for a grading layer of GaInAs/GaAs and low-bandgap cells in AlGaInAs/GaInAs/GaAs.

Task 2. Develop and demonstrate inter-cell tunnel junction contacts in the higher bandgap AlGaInAs alloys.

Task 3. Develop and demonstrate technology for a higher bandgap concentrator cell in AlGaInAs alloys.

## **DISCLAIMER**

**This report was prepared as an account of work sponsored by an agency of the United States Government. Neither the United States Government nor any agency thereof, nor any of their employees, makes any warranty, express or implied, or assumes any legal liability or responsibility for the accuracy, completeness, or usefulness of any information, apparatus, product, or process disclosed, or represents that its use would not infringe privately owned rights. Reference herein to any specific commercial product, process, or service by trade name, trademark, manufacturer, or otherwise does not necessarily constitute or imply its endorsement, recommendation, or favoring by the United States Government or any agency thereof. The views and opinions of authors expressed herein do not necessarily state or reflect those of the United States Government or any agency thereof.**

---

## **DISCLAIMER**

**Portions of this document may be illegible in electronic image products. Images are produced from the best available original document.**

Task 4. Demonstrate a complete two-gap monolithic concentrator cell with AM2 efficiency of 28% or more.

Task 5. Investigate the potential of AlInAsSb alloys grown on InAs substrates.

#### Short Summary

The progress made on the above tasks is summarized below.

Task 1. Several  $\text{Ga}_{1-x}\text{In}_x\text{As}$  graded layers with  $x = .10$  final layers have been grown by continuous linear grading. Surface morphology, etch pit densities and photoluminescence have been characterized for these layers.

Extensive doping characterization of  $x = .10$  and  $.20$   $\text{Ga}_2\text{In}_{1-x}\text{As}$  using both DEZn and  $\text{H}_2\text{Se}$  has been made.

Task 2. Extensive characterization of the doping behavior of  $\text{H}_2\text{Se}$  and DEZn in GaAs under various growth conditions has been done with the goal of obtaining working tunnel junction in GaAs. The work has pointed future directions to obtain a tunnel junction.

Task 3. The first AlGaInAs layer with good surface morphology has been obtained. The conditions that led to this, as well as future plans, will be discussed in detail below.

Task 4. This task is in progress by way of work on Tasks 1, 2, and 3 above.

Task 5. Because of the heavy attention devoted to the doping problems and AlInGaAs, work on this task has been deferred.

## DETAILED DISCUSSION

### Task 1: GaInAs Growth

#### a) Grading

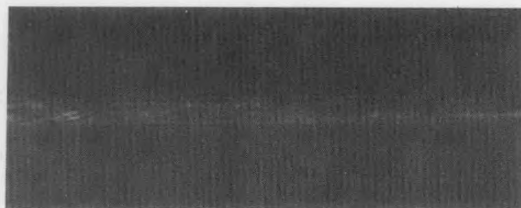
Several graded  $\text{Ga}_{1-x}\text{In}_x\text{As}$  layers on GaAs substrates have been grown and characterized. The layers were grown at 600°C. A short GaAs buffer layer was grown first (5 min.). The graded layer was grown by linearly changing the TMIn flow upwards and simultaneously decreasing the TMGa flow, while keeping the nominal  $[\text{TMGa} + \text{TMIn}]$  flux = 34  $\mu\text{mole}/\text{min}$ . Because the TMIn flow controller has a minimum setting of 10 sccm, the initial step is ~1% InAs in the solid. This is the only abrupt change in solid composition. A constant composition layer is grown on top of the grading layer for ~0.5  $\mu\text{m}$ . Characterization was by surface morphology, photoluminescence, and etch pit densities.

Figure 1 shows the surface and cross sections of three representative layers. Each was grown as described, with only the grading rate changed. The first was grown at  $10.5\%/\mu\text{m}$ , the second at  $5\%/\mu\text{m}$ , and the last at  $4\%/\mu\text{m}$ . All three layers have an end composition of 10%. The growth rate was  $\sim 0.044 \mu\text{m}/\text{min}$ . for all the layers.

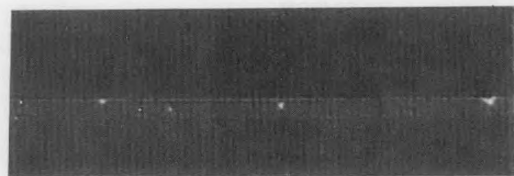
As expected, the surface morphology improved greatly as the grading rate was decreased. The  $10\%/\mu\text{m}$  shows a large density of hillocks bounded by  $\langle 111 \rangle$  planes. The  $5\%/\mu\text{m}$  layer showed only a few scattered hillocks, and the  $4\%/\mu\text{m}$  layer was about totally free of hillocks. Since the final composition was 10% in all cases, the etch pit density (EPD) was expected to be  $\leq 10^4 \text{ cm}^{-2}$ , or equivalent to the substrate EPD.<sup>1</sup> This was the case. There is little difference between the photoluminescence spectra of the 10 and  $4\%/\mu\text{m}$  samples, both in intensity and half widths. This supports the conclusion that few dislocations are propagated into the epitaxial layer for  $x \leq .10$ , but that the surface morphology is dramatically affected.

Figure 1  
GRADED  $\text{Ga}_{1-x}\text{In}_x\text{As} / \text{GaAs}$  (  $x = .10$  )

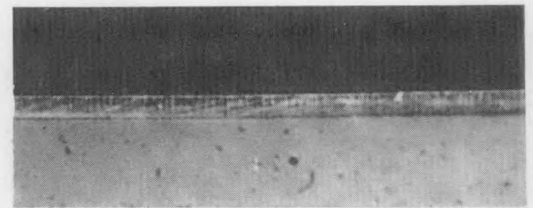
10.5%/ $\mu\text{m}$



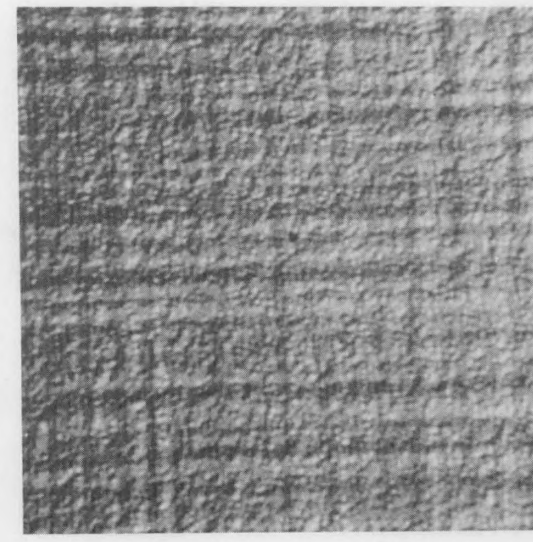
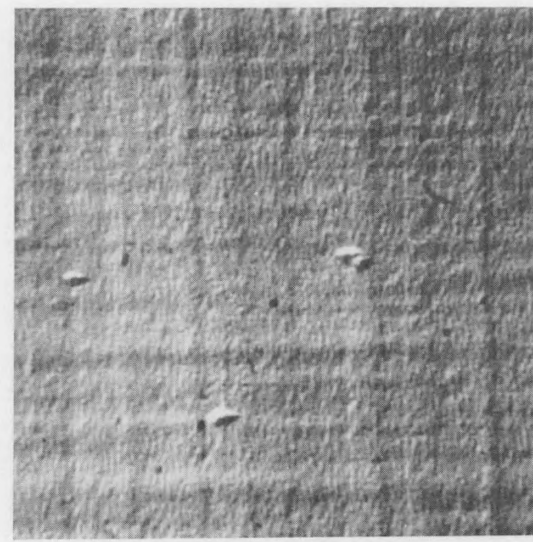
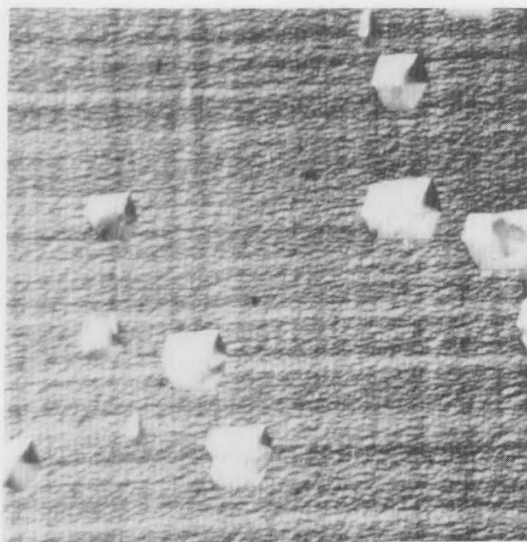
5.1%/ $\mu\text{m}$



4.3%/ $\mu\text{m}$



4



20  $\mu\text{m}$

b) Doping

Both n-type and p-type doping in  $\text{Ga}_{1-x}\text{In}_x\text{As}$   $x = .10$  and  $x = .20$  have been studied during the last quarter. The most complete characterization has been the n-type dopant Se, using  $\text{H}_2\text{Se}$  as the carrier gas. Figures 2 through 9 show the various doping and mobility data at 300 and 77°K for  $\text{Ga}_{1-x}\text{In}_x\text{As:Se}(x=.10, .20)$ .

For  $x = .10$   $\text{Ga}_{1-x}\text{In}_x\text{As}$  grown at 600°C, Se doping levels between  $1 \times 10^{18} \text{ cm}^{-3}$  and  $2.5 \times 10^{19} \text{ cm}^{-3}$  have been achieved controllably for 48 ppm  $\text{H}_2\text{Se}$  in  $\text{H}_2$  flows between 4 and 32 sccm. The background (no  $\text{H}_2\text{Se}$ ) doping was measured at  $n \sim 8 \times 10^{16} \text{ cm}^{-3}$  (C-V method). The doping levels do not change significantly between 300°K and 77°K, indicating that few if any deep levels are involved. Concentrations between  $1 \times 10^{17}$  and  $1 \times 10^{18} \text{ cm}^{-3}$  may be reached, it is believed, by substituting a  $\text{H}_2\text{Se}$  tank of lower concentration (~25 ppm) or controlling the flow below 1 sccm. The 300°K Hall mobilities vary from 600 to 2630  $\text{V-sec/cm}^2$  between  $2.5 \times 10^{17}$  and the background of  $8 \times 10^{16} \text{ cm}^{-3}$ . This compares to theoretical drift mobilities in GaAs of ~1000 to 5000 over the same range.<sup>2</sup> The 77°K mobilities vary from 1100 to 4700  $\text{V-sec/cm}^2$  over the same range.

For  $x = 0.20$   $\text{Ga}_{1-x}\text{In}_x\text{As}$  grown at 600°C, Se doping levels between  $2 \times 10^{17}$  and  $1.4 \times 10^{19} \text{ cm}^{-3}$  have been achieved controllably for 48 ppm  $\text{H}_2\text{Se}$  flows between 4 and 32 sccm. The background doping appears to be  $n \sim 1 \times 10^{16} \text{ cm}^{-3}$ , although there is difficulty in making reliable ohmic contacts to this material, so that the van der Pauw readings have significant error associated with them. As with the 10% material, the doping levels do not change significantly between 300°K and 77°K, and concentrations between  $1 \times 10^{16}$  and  $1 \times 10^{17} \text{ cm}^{-3}$  may be reached, it is believed, by either using a lower  $\text{H}_2\text{Se}$  in  $\text{H}_2$  concentration or controlling the

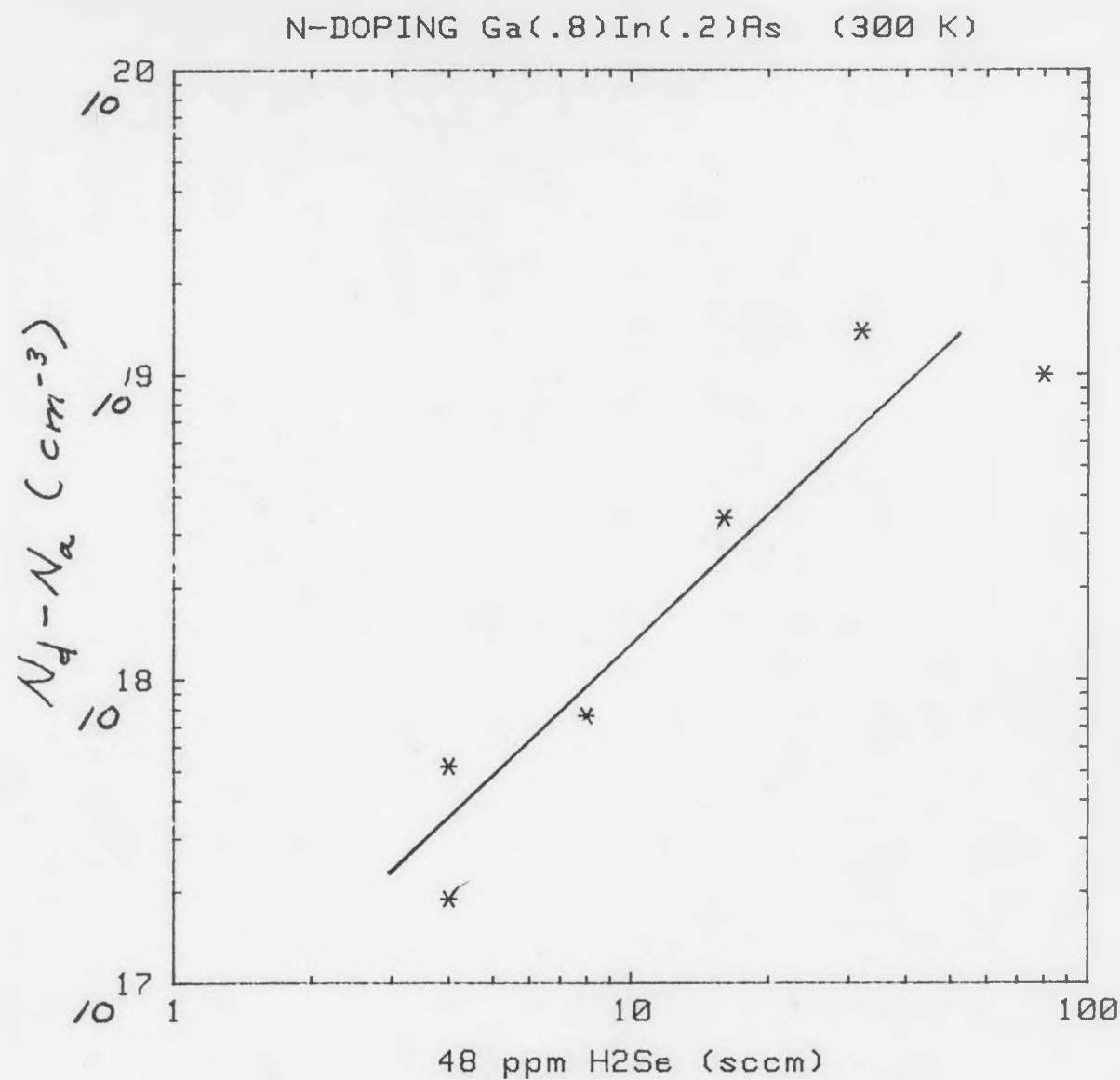


Fig. 2  $N_d - N_a$  vs H<sub>2</sub>Se flow for 20% GaInAs at 300°K.

7

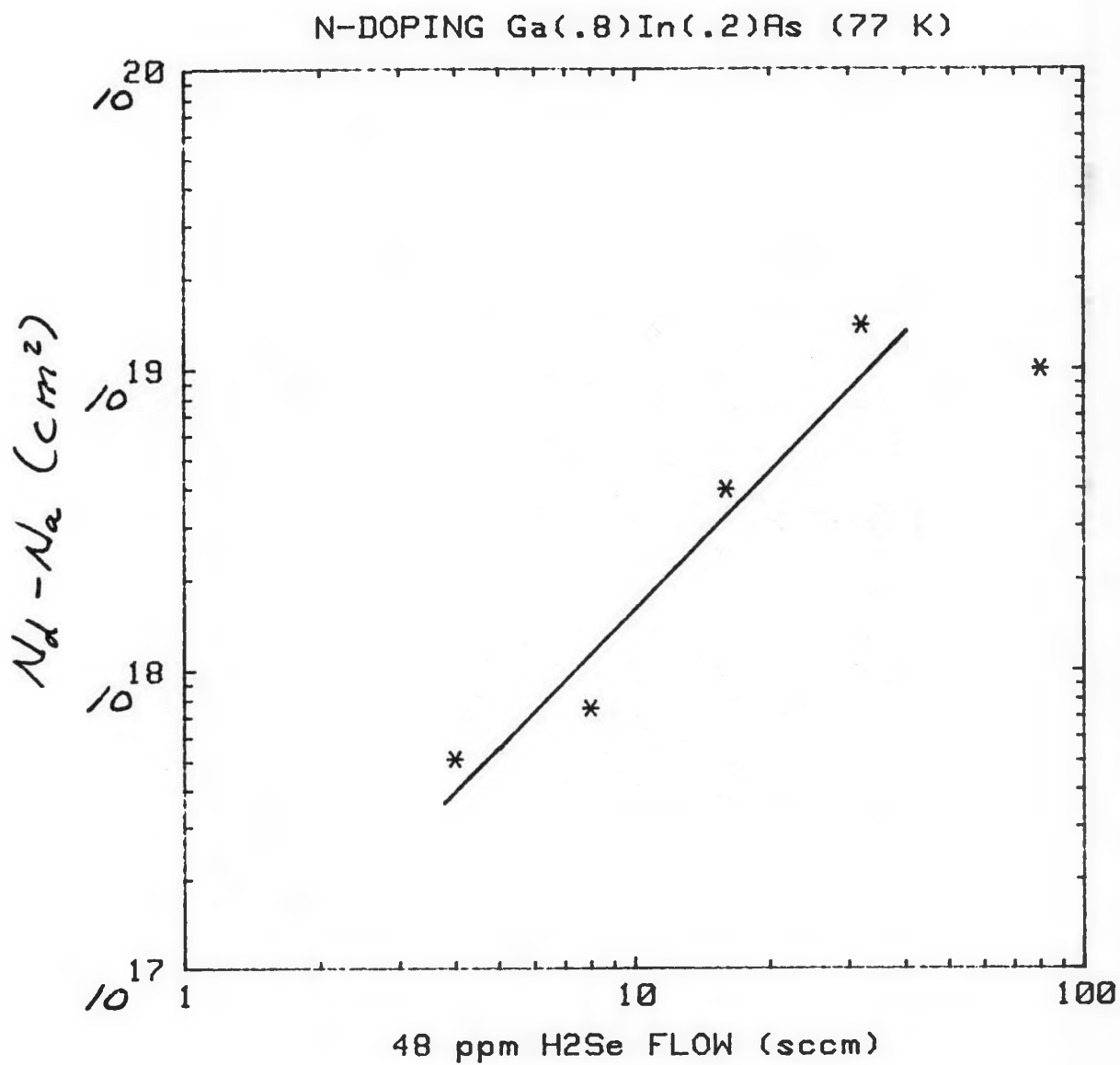


Fig. 3  $N_d - N_a$  vs H<sub>2</sub>Se flow for 20% GaInAs at 77°K.

MOBILITY VS DOPING Ga(.8)In(.2)As (300 K)

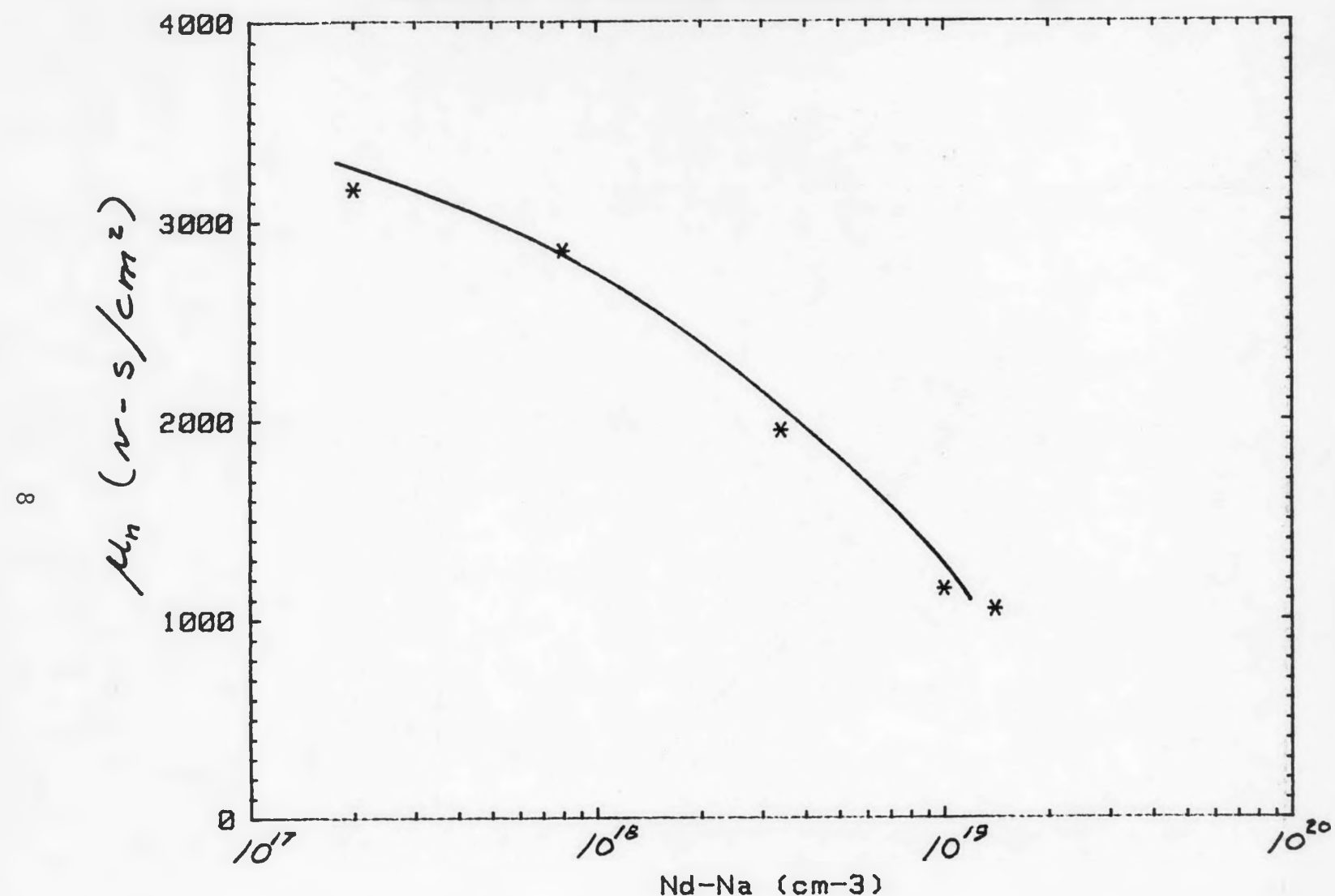


Fig. 4 Mobility vs  $N_d - N_a$  for 20% GaInAs at 300°K.

MOBILITY VS DOPING Ga(.8)In(.2)As (77 K)

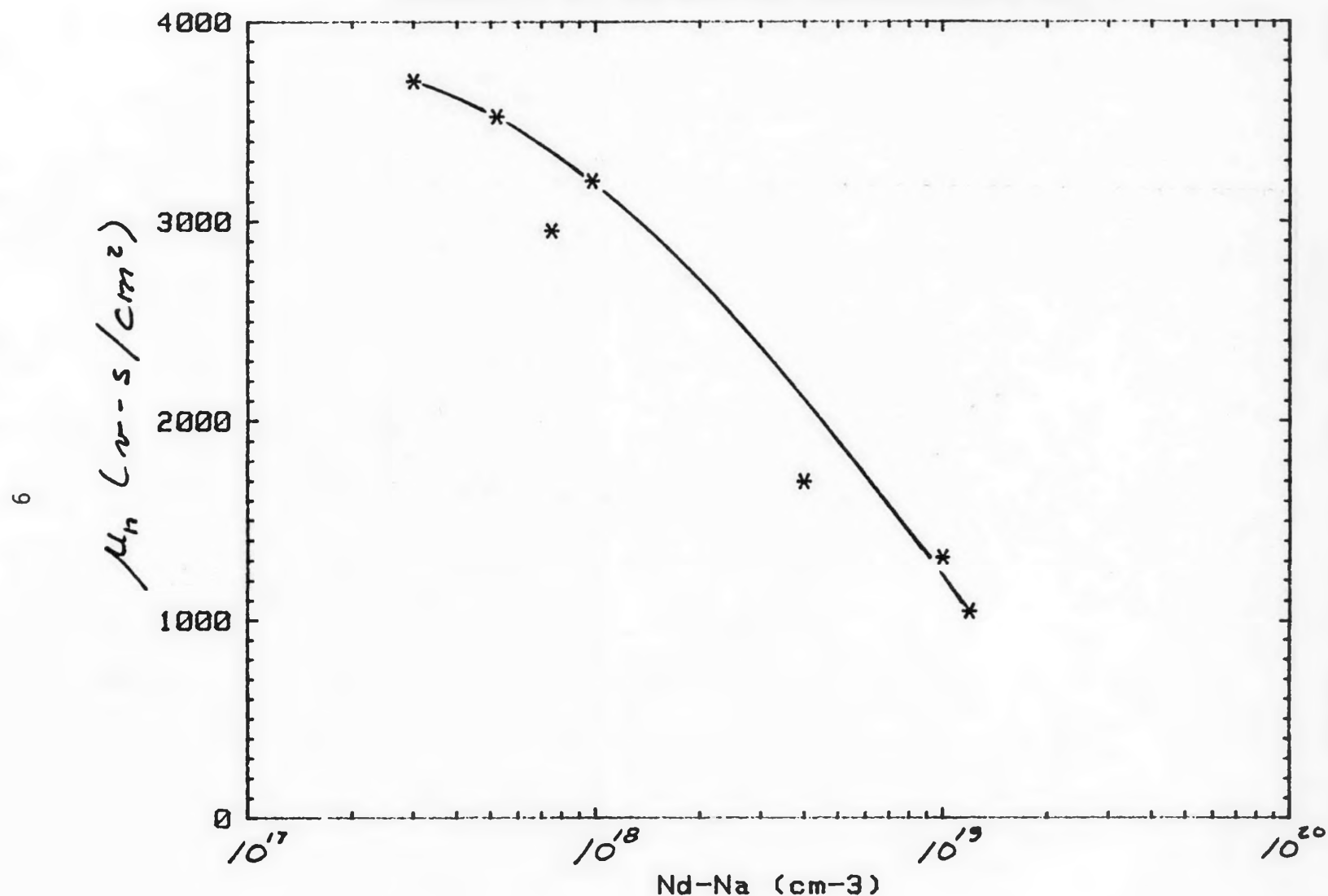


Fig. 5 Mobility vs  $N_d - N_a$  for 20% GaInAs at 77°K.

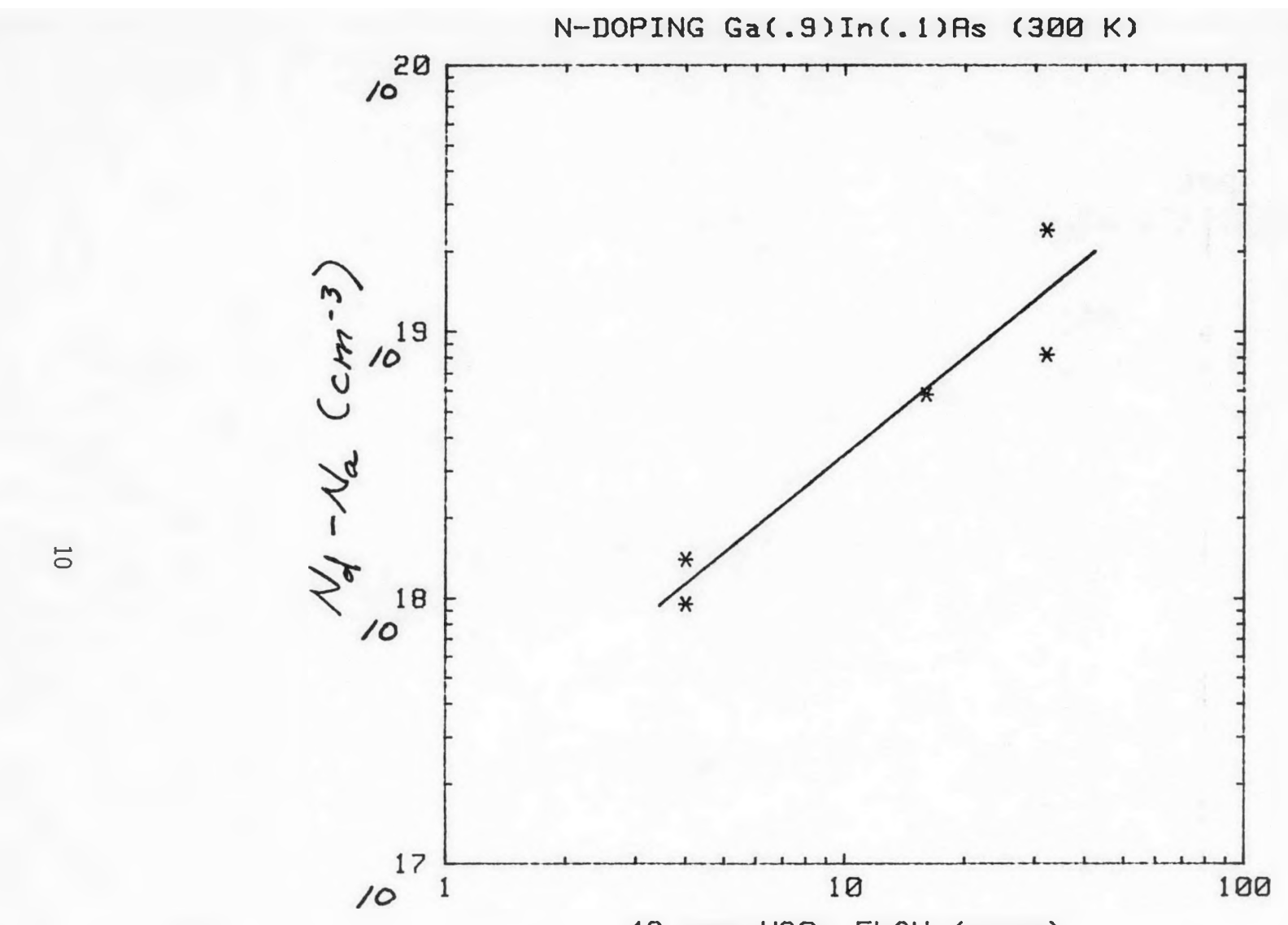


Fig. 6  $N_d - N_a$  vs  $\text{H}_2\text{Se}$  flow for 10% GaInAs at 300°K.

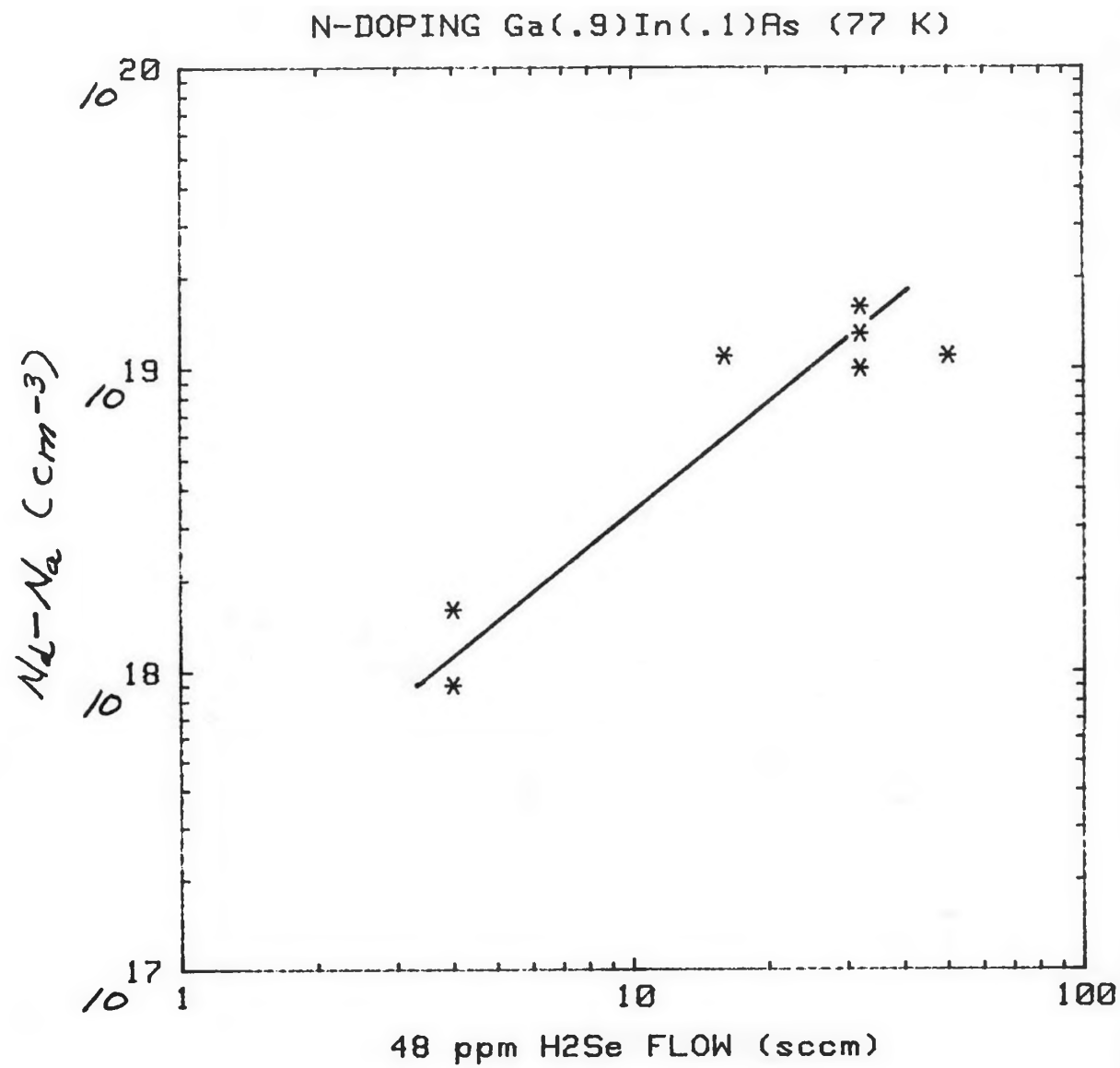


Fig. 7  $N_d - N_a$  vs H<sub>2</sub>Se flow for 10% GaInAs at 77°K.

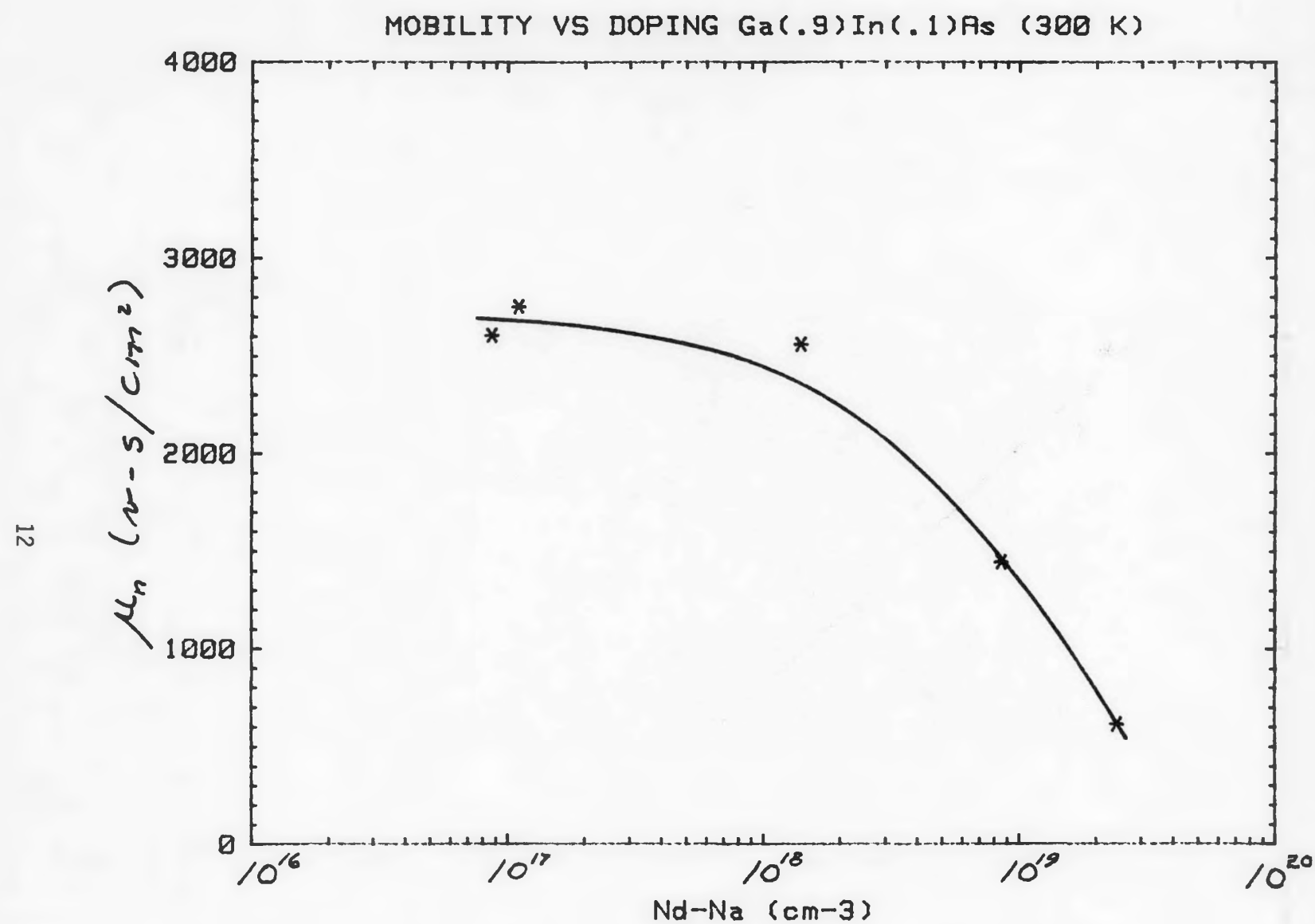


Fig. 8 Mobility vs  $N_d-N_a$  for 10% GaInAs at 300°K.

13

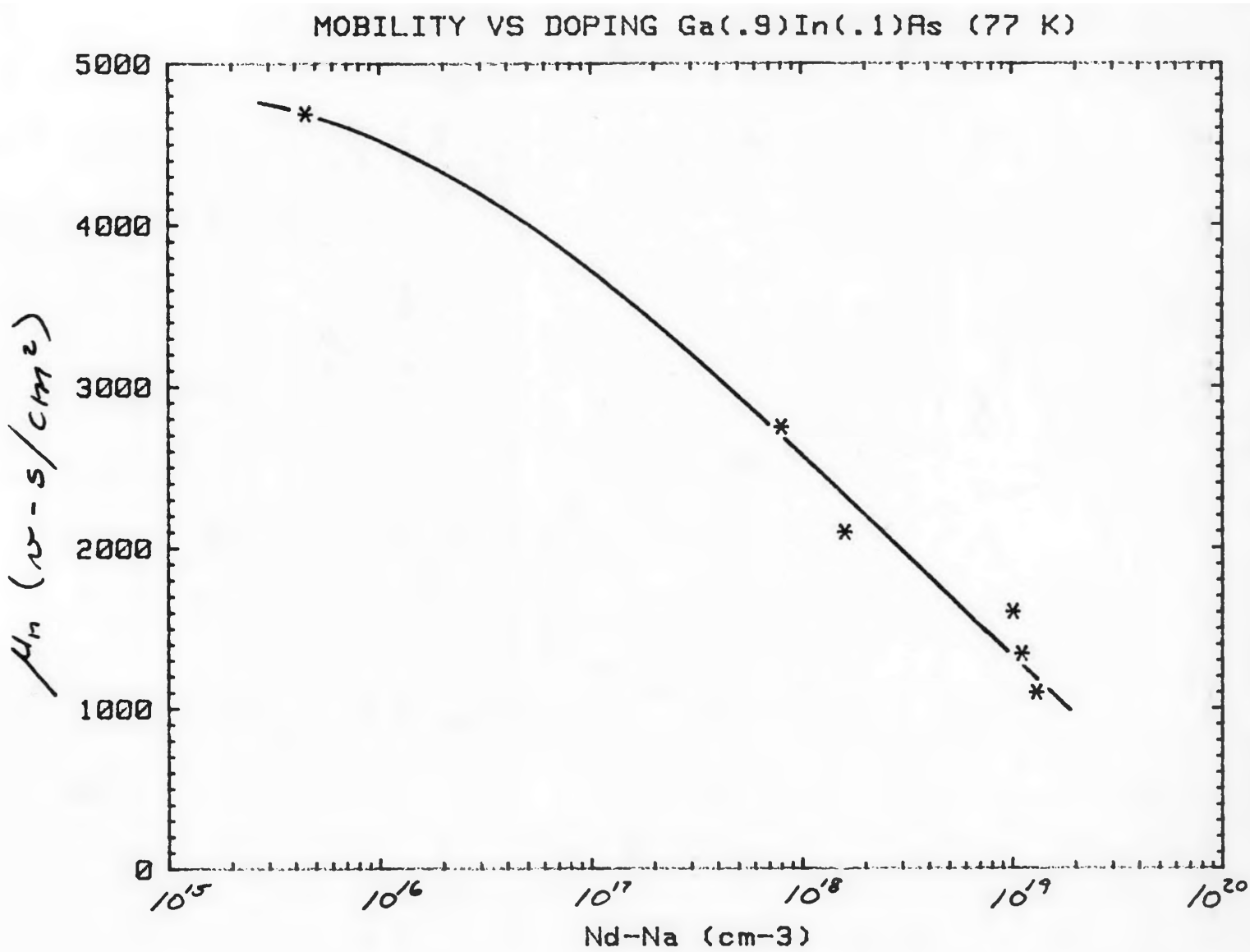


Fig. 9 Mobility vs  $N_d - N_a$  for 10% GaInAs at 77°K.

flow to below 1 sccm. The 300°K Hall mobilities vary from 1050 to 3160  $\text{cm}^2/\text{V}\cdot\text{sec}$  over the doping range  $1.4 \times 10^{19}$  to  $2 \times 10^{17} \text{ cm}^{-3}$ . This compares to  $\sim 1500$  to  $4000 \text{ cm}^2/\text{V}\cdot\text{sec}$  for GaAs.<sup>2</sup>

The studies of p-type dopants in GaInAs has not been as extensive. Figure 10 shows a plot of  $N_A - N_D$  (van der Pauw) vs DEZn mole fraction in the gas phase, at a growth temperature of 600°C. Hole concentrations are controllable from  $4.5 \times 10^{18}$  to  $4 \times 10^{19} \text{ cm}^{-3}$ . The lowest point represents the lowest DEZn flux (1 sccm at -25°C bubbler temperature) possible on the current system. The extremely high Zn concentration in the crystal is attributable to the low (600°C) growth temperature, since Zn incorporation has been experimentally determined to be proportional to  $[p_{\text{Zn}}]^{-2}$ , where  $p_{\text{Zn}}$  is the elemental vapor pressure of Zn. Two points grown with DECd are shown also for comparison. Paradoxically, higher DECd flows appear to produce lower dopings. This is probably because the DECd is not electronic grade, and more n-type impurities are carried to the deposition zone at higher flows. The high level of Zn in the crystal coupled with the tendency of Zn to diffuse rapidly at high concentrations is responsible for degrading the junction quality. Junctions grown in  $x = .10 \text{ Ga}_{1-x}\text{In}_x\text{As}$  have shown low (~1v) reverse breakdown voltages (Fig. 11).

The effects of changing the V/III ratio on background doping for GaAs grown with TMAs has been studied. It is believed that similar results apply to the ternary alloy  $\text{Ga}_{1-x}\text{In}_x\text{As}$ , at least for low In ( $x \leq .20$ ) compositions. Figure 12 shows a plot of the background (undoped) carrier concentrations as a function of the V/III ratio, and also the associated mobilities. There does not seem to be any systematic variation of background doping with the TMAs/TMGa ratio, nor does the 300°K Hall mobility show any systematic variation. It is concluded that the background doping in GaAs grown with TMAs is n-type, is carried by the TMAs,

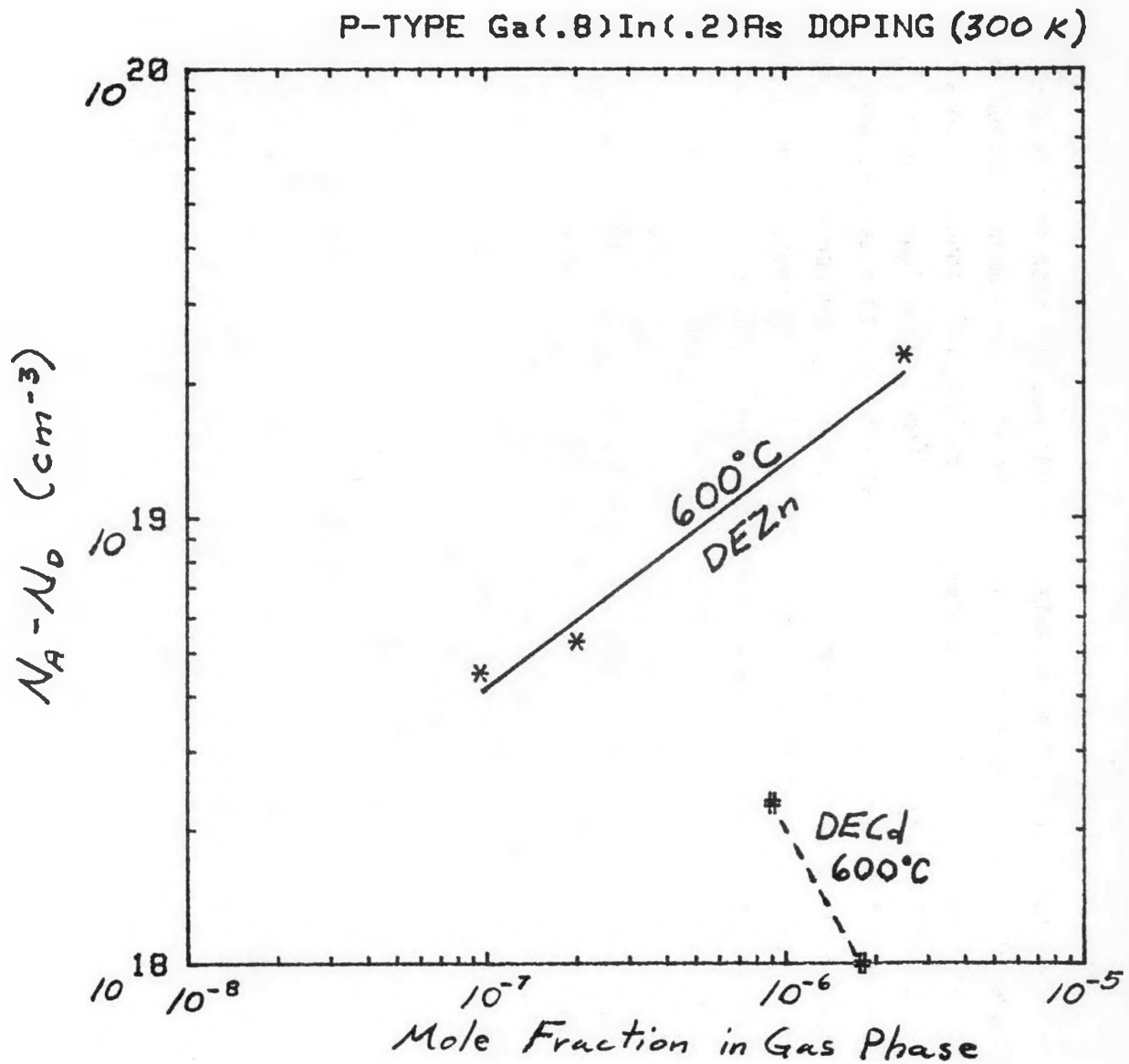
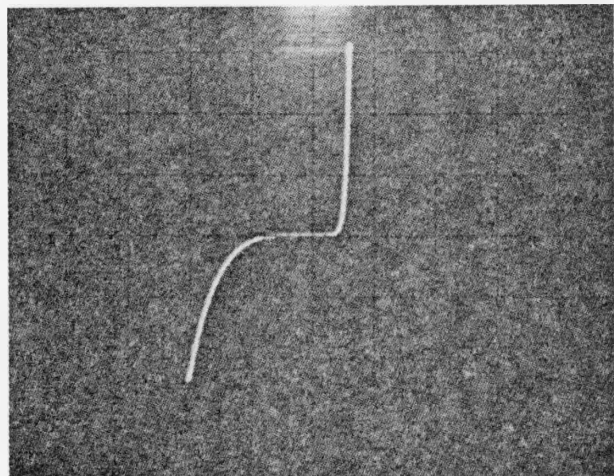


Fig. 10  $N_a - N_d$  vs mole fraction in gas phase of DEZn or DECd at 300°K.

**Ga<sub>0.90</sub>In<sub>0.10</sub>As/GaAs P-N JUNCTION**



HORIZONTAL 1 V/DIV.  
VERTICAL 1 mA/DIV.

Fig. 11 I-V tract of Ga<sub>0.90</sub>In<sub>0.10</sub>As p/n junction growth with Zn and Se dopants.

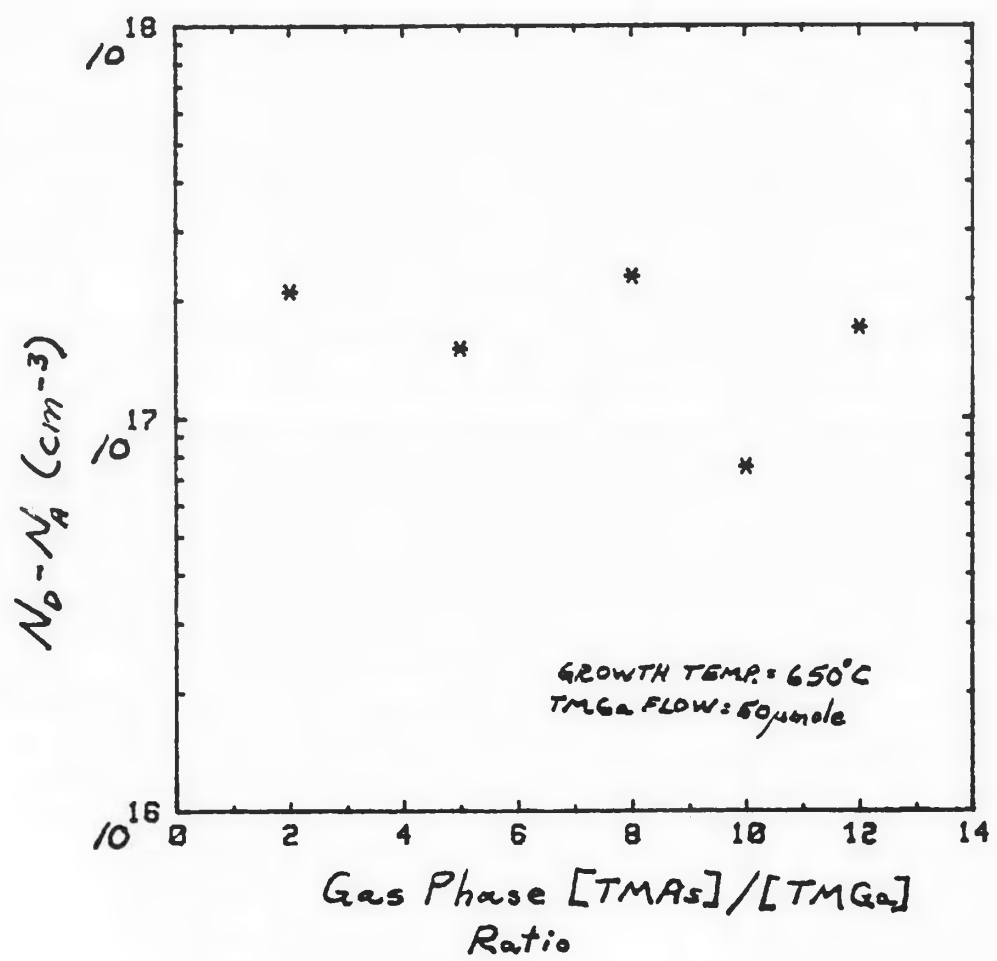
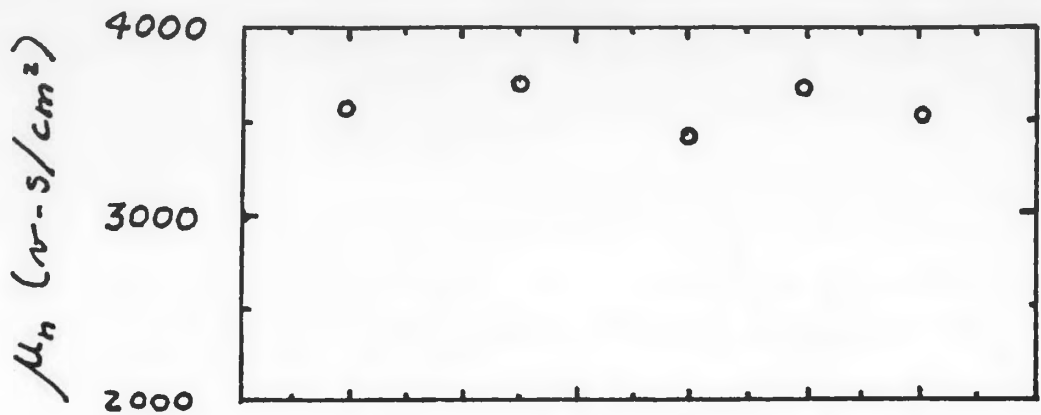


Fig. 12 Background doping and mobility in GaAs grown using TMAs at various ratios of TMAs/TMGa. Growth temperature was 650°C and TMGa was held constant at 50 μmole/min.

and that the contaminant incorporation does not depend upon the TMAs concentration.

### Task 2: Tunnel Junction

Data was taken on diodes grown during the previous quarter. Capacitance-voltage measurements on these GaAs p/n junctions indicate that the n-side doping is  $6 \times 10^{17} \text{ cm}^{-3}$ , somewhat lower than that indicated by van der Pauw data. The zero bias depletion width is 400-500 Å. This width is still too large for effective tunneling. It is felt that by increasing the n-side doping, the zero bias depletion width will shrink to  $\sim 150/200$  Å. A more detailed study of n- and p-doping in GaAs was initiated pursuant to these goals. The target goal is a GaAs p/n junction with  $n \sim 1 \times 10^{20} \text{ cm}^{-3}$  and  $p \sim 1 \times 10^{19} \text{ cm}^{-3}$ , with minimum spread in the metallurgical junction due to p-dopant diffusion. The difficulties to date have centered around obtaining Se-doping above  $10^{17} \text{ cm}^{-3}$  and Zn-doping below  $10^{19} \text{ cm}^{-3}$ .

Figures 13 and 14 show the results to date of the n- and b-doping studies. Figure 13 shows a plot of  $N_D - N_A$  (van der Pauw measurements) vs  $\text{H}_2\text{Se}$  flow (48 ppm in  $\text{H}_2$ ) for two growth temperatures, 625 and 650°C. The 625-650°C range was chosen for two reasons; first, Zn diffusion problems will be minimized at the lower growth temperatures, which corresponds to nearly the lowest limit for GaAs growth, and second, this temperature range is the most likely range for GaInAlAs growth. There is a difference in Se incorporation between the two temperatures, with higher electron concentrations being achieved at 625°C at flows above 25 sccm. Control between  $n \sim 1 \times 10^{17}$  to  $4.5 \times 10^{18} \text{ cm}^{-3}$  has been achieved. At present, 200 sccm represents the upper limit on  $\text{H}_2\text{Se}$  flow, and a higher (and more stable) 200-ppm concentration of  $\text{H}_2\text{Se}$  has been placed on order. Since the curves of Fig. 14 do not saturate at higher flows, it is believed that even higher doping can still be achieved using Se.

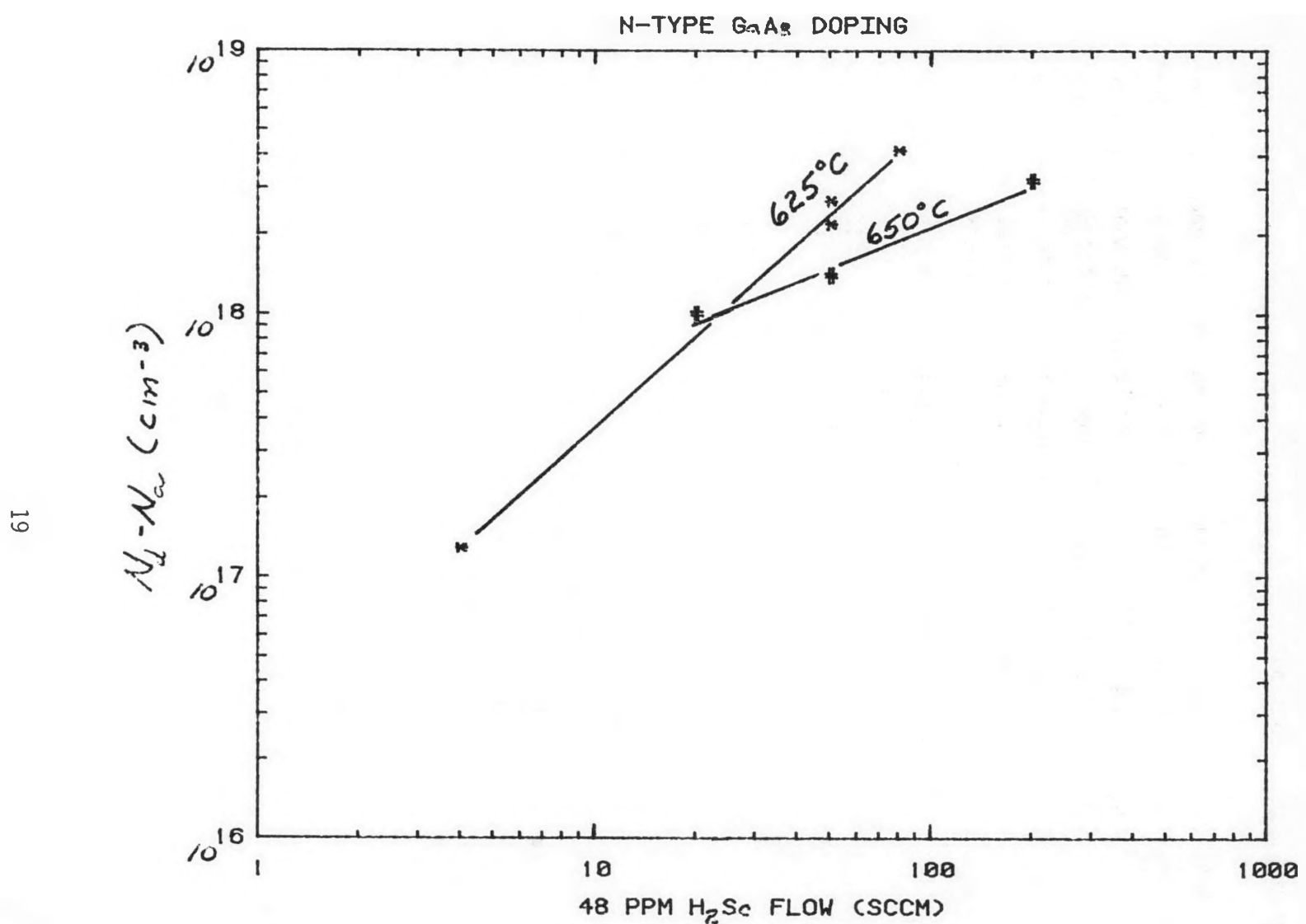


Fig. 13  $N_d - N_a$  vs  $\text{H}_2\text{Se}$  flow for GaAs grown with  $\text{AsH}_3$  at 625 and 650°C.

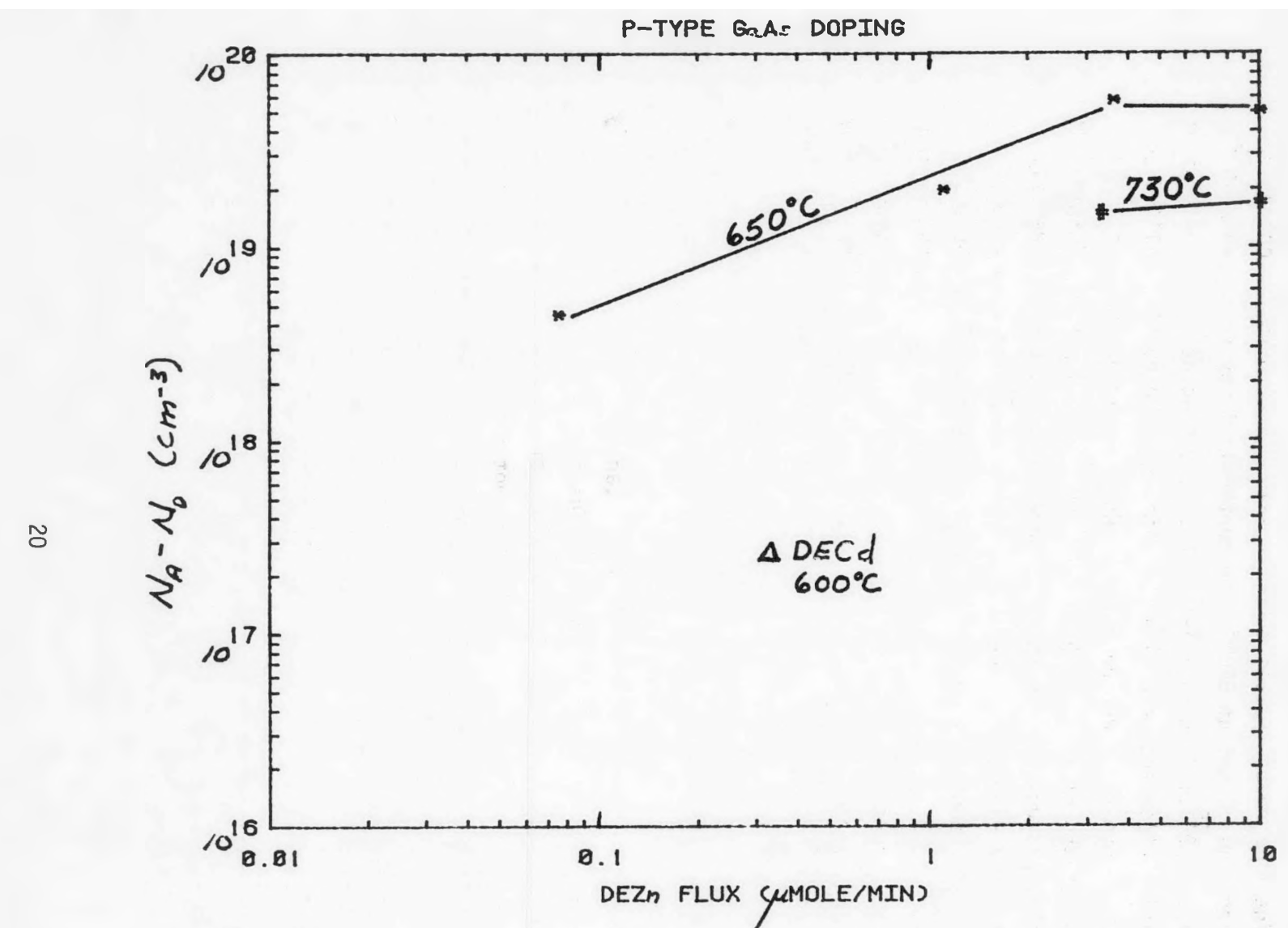


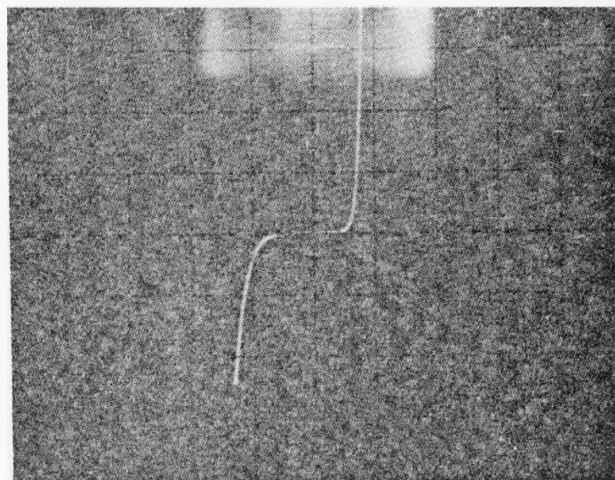
Fig. 14  $N_a - N_d$  vs DEZn flux for GaAs grown with  $\text{AsH}_3$  at 650 and 730°C.  
One point obtained from DECd is shown also.

Figure 14 shows a plot of  $N_A - N_D$  (van der Pauw) vs DEZn flux in micromoles in the growth tube. Again, two growth temperatures are indicated, and in addition, one data point from DECd doping is indicated. The hole concentration tends to saturate at DEZn concentrations above 3  $\mu\text{mole}/\text{min.}$ , but at 650°C some controllability from  $p \sim 5 \times 10^{19}$  down to  $4.5 \times 10^{18} \text{ cm}^{-3}$  is achieved. This lowest point is representative of the minimal flow possible (1 sccm) with the DEZn bubbler chilled to -25°C (just above the freezing point). While lower doping levels have been demonstrated at 730°C (e.g.,  $p \sim 10^{17} \text{ cm}^{-3}$  at 0.1  $\mu\text{mole DEZn}/\text{min}$ ), it is felt that diffusion of Zn at the higher temperature will seriously degrade a tunnel junction. The DECd point is shown for comparison. This point represents a relatively high flow (25 sccm) with the DECd bubbler at 15°C. Increased flow would probably not increase the doping significantly, and certainly not to the levels required for a tunnel junction. Paradoxically, another run at twice the DECd flow resulted in an order of magnitude lower doping. A possible explanation is that the DECd has a very low vapor pressure, causing poor saturation of the  $\text{H}_2$  carrier with DECd vapor. Also, the sample used was not electronic grade and the material may be somewhat compensated.

In summary, the DEZn doping at 650°C can be controlled sufficiently to create a tunnel junction. The Zn diffusion may be dealt with by increasing the n-side doping about an order of magnitude above that of the p-side, so that the diffusing Zn does not significantly compensate the n-side of the junction and thus widen the zero bias depletion width.

Figure 15 shows an I-V trace of a GaAs p/n junction grown using the maximum attainable Se doping ( $3 \times 10^{18} \text{ cm}^{-3}$ ) with moderately high p-doping ( $2 \times 10^{19} \text{ cm}^{-3}$ ). The reverse breakdown voltage is ~1/volt, and is characteristic of tunnel breakdown mechanisms rather than avalanche mechanisms. True tunneling characteristics are expected when higher Se levels are achieved.

OM-VPE GaAs p/n JUNCTION



HORIZONTAL 1 volt/div.  
VERTICAL 0.2 mA/div.  
GaAs GROWTH TEMP. = 625°C  
DOPING  $p \sim 2 \times 10^{19} \text{ cm}^{-3}$   
 $n \sim 3 \times 10^{18} \text{ cm}^{-3}$

Fig. 15 I-V tract of GaAs p/n junction grown with Se and Zn dopants:  
 $n \sim 3 \times 10^{18}$  and  $p \sim 2 \times 10^{19} \text{ cm}^{-3}$ .

### Task 3: AlGaInAs Materials Development and High-Gap Cell

Using the information learned during the last quarter concerning susceptor cleanliness, etc., further attempts at growing AlGaInAs have been made. By rigorously baking out the SiC-coated susceptors and paying strict attention to elimination of low level contaminants in the reactor tube, AlGaInAs wafers with good morphology (specularly reflective surface) have now been grown. Electron beam microprobe data indicates the relative Al:Ga:In ratios to be 0.12, .72, and .16, respectively (uncorrected). Conceptually, the growth was treated as a GaInAs run with Al substituted for 11% of the [Ga+In] in the gas phase. Although the cross section of the layer showed some strain, this is because no graded layer was used. Future efforts will be directed at increasing the Al content.

One attempt was made to fabricate an AlGaAs (1.7 eV) solar cell, but the junction exhibited very low short-circuit currents. It is felt that the doping levels were too high. Reasonably good p/n junctions (small area) have been fabricated, however, in this material (e.g., see Quarterly Report No. 3, Fig. 7).

### Task 4: Complete Structure

This task is in progress by way of progress on the above 3 tasks.

### Task 5: Evaluation of AlInAsSb/InAs

Work on this task has been deferred to make more reactor time available for the above tasks.

## PLANS FOR THE FIFTH QUARTER

During the next quarter, the plans are:

Task 1: Optimize  $\text{Ga}_{1-x}\text{In}_x\text{As}$  p/n junctions:

1. Finish characterizing p-doping and control to lower limits.
2. Fabricate and test 1.15-eV cells.

Task 2: Continue development of tunnel junction:

1. Increase obtainable Se doping levels in GaAs.
2. Demonstrate small-area tunnel junction.
3. Extend to 1.7 eV AlGaAs.

Task 3: High-gap Cell:

1. Optimize 1.7-eV cell structure.
2. Explore phase diagram for AlGaInAs.
3. Characterize p- and n-doping in AlGaAs, AlGaInAs .

Task 5: Evaluation of AlInAsSb/InAs

1. Continue examination of InAsSb growth.

### REFERENCES

1. G. H. Olsen and M. Ettenberg, Crystal Growth 2, 1 (1978).
2. S. M. Sze, Physics of Semiconductor Devices (Wiley & Sons, New York), p. 40.